Continental Shelf Research 69 (2013) 88–100

Contents lists available at ScienceDirect

Continental Shelf Research

journal homepage: www.elsevier.com/locate/csr

Research papers

Distribution and abundance of rippled scour depressions along the California coast

Alexandra C.D. Davis [a,1], Rikk G. Kvitek [a,*], Craig B.A. Mueller [a], Mary A. Young [a], Curt D. Storlazzi [b], Eleyne L. Phillips [b]

[a] Seafloor Mapping Lab, California State University Monterey Bay, 100 Campus Center, Seaside, CA 93955, USA
[b] U.S. Geological Survey, Pacific Science Center, 400 Natural Bridges Drive, Santa Cruz, CA 95060, USA

ARTICLE INFO

Article history:
Received 1 December 2012
Received in revised form
10 September 2013
Accepted 12 September 2013
Available online 23 September 2013

Keywords:
Bedforms
Continental shelf
Benthic habitat
Marine protected area (MPA)
Marine spatial planning
Seafloor mapping

ABSTRACT

Rippled scour depressions (RSDs) are prominent sediment features found on continental shelves worldwide. RSDs are generally characterized as elongate nearshore deposits of coarser-grained sediment with long-wavelength bedforms depressed 0.4–1.0 m below the surrounding finer-grained sediment plateau, thereby adding complexity and patchiness to relatively homogeneous unconsolidated sedimentary substrates on the inner continental shelf. Most research corroborates the hypothesis that RSDs are formed and maintained by currents and wave interaction with the seafloor sediment. While many localized studies have described RSDs, we use bathymetric and acoustic backscatter data from the statewide California Seafloor Mapping Program (CSMP) to describe the spatial distribution of RSDs at the regional scale. The goals were to: (1) quantify the abundance and patterns of distribution of RSDs along the entire 1200 km California coast, and (2) test the generality of previously described or predicted relationships between RSD occurrence and geographic, oceanographic and geomorphic parameters, including depth, wave energy, latitude, shelf width, and proximity to bedrock reefs and headlands. Our general approach was to develop and apply a Topographic Position Index-based (TPI) landscape analysis tool to identify the distinct edges of RSDs in bathymetry data to differentiate the features from other sedimentary and rocky substrates. Spatial analysis was then used to quantify the distribution and abundance of RSDs and determine the percentage of bedrock reef, sedimentary and RSD substrates on the continental shelf within state waters. RSD substrate accounted for 3.6% of the California continental shelf, compared to 8.4% for bedrock reef substrate. The percent coverage of RSD substrate varied with depth, with 88% occurring in the 20–80 m depth range, and increased with proximity to bedrock reef substrate. RSD cover also varied significantly with shelf width, but not with proximity to headlands. Given the recent findings on the ecological significance of RSD, the results are relevant to marine spatial planning and ecosystem based management in terms of evaluating how well the 68 individual marine protected areas (MPAs) within California's newly designated state-wide MPA network collectively represent regional percentages of bedrock, sedimentary, and RSD substrate.

1. Introduction

Coarse-grained sediment features termed, “rippled scour depressions” (RSDs) (Cacchione et al. 1984) have been identified and described worldwide (e.g., Reimnitz et al., 1976; Cacchione et al., 1984; Auffret et al., 1992; Murray and Thieler, 2004; Ferrini and Flood, 2005; Garnaud et al., 2005; Holland and Elmore, 2008; Iacono and Guillen, 2008; Bellec et al., 2010). These studies describe RSDs as variable in shape and size, but typically elongate and oriented normal to shore, and ranging in size from 10 s to 100 s of m in width and up to 3 km in length. While RSDs have been most commonly reported as occurring in depths of 5 m to 80 m, they have also been identified down to 160 m (Bellec et al., 2010), and can occur as singular entities or in clusters of multiple features. The depressions are typically 0.4–1.0 m deeper and coarser-grained (0.3–1.0 mm) than the sediment on the surrounding seabed (0.05–0.30 mm) (Fig. 1). RSDs also characteristically contain larger ripples (0.5–1 m wavelength) than found on the surrounding sediment (Bagnold, 1946) (Fig. 1).

While there is general consensus on the characteristic geomorphology and physical properties of RSDs, there is ongoing speculation regarding the mechanisms and environmental parameters governing where and how RSDs form. Cacchione et al. (1984)

* Corresponding author. Tel.: +1 831 582 3529.
E-mail address: rkvitek@csumb.edu (R.G. Kvitek).
[1] Present address: Department of Zoology, Oregon State University, 3029 Cordley Hall Corvallis, OR 97331, USA.

0278-4343/$ - see front matter © 2013 Elsevier Ltd. All rights reserved.
http://dx.doi.org/10.1016/j.csr.2013.09.010

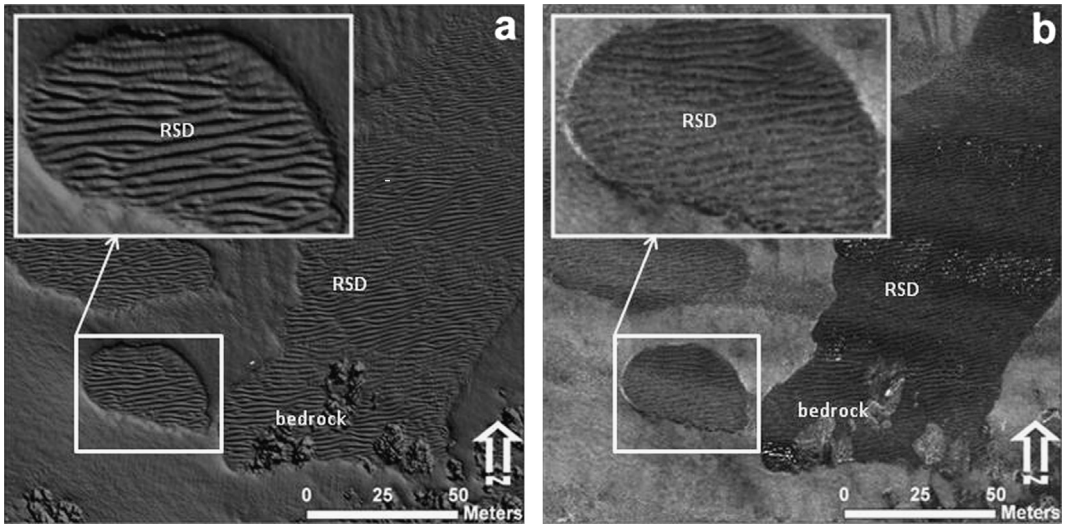

Fig. 1. Example image from geophysical data of rippled scour depressions (RSDs) and patches of bedrock reef surrounded by fine sediment plateau. (a) Shaded relief digital elevation model (DEM) raster derived from multibeam bathymetry data illustrates distinct depression boundaries and larger sand waves of the RSDs. (b) Acoustic backscatter image showing the coarser-grained sediment of the RSDs as areas of stronger (darker) acoustic return. Inserts are close-up views of RSD ripples.

suggest that the winnowing or scouring of finer-grained surficial sediment through storm-induced bottom currents forms the features. These currents are redirected in the cross-shore direction by local topographic features such as rock ledges. Consistent with this hypothesis, other studies have found RSDs associated with rock outcrops (Auffret et al., 1992), and bathymetric highs of consolidated relict sediment (Aubrey et al., 1984; Garnaud et al., 2005). Cacchione et al. (1984) also attributed storm-induced waves as a mechanism for the formation of the large ripples inside the depression.

Cacchione et al. (1987) described fine grain crescentic dunes within the RSDs that appeared to be slowly migrating obliquely to the shelf gradient. These dunes are larger and more abundant the shallower the depth and eventually coalesce close to shore. They hypothesized that the dunes were a potential source of sediment that eventually supply muddy deposits on the central shelf. Additionally, though these dunes are active, they are moving at a rate that is only detectable on the decadal scale (Cacchione et al. 1987; Seafloor Mapping Lab at CSUMB: SFML Data Library, 2011). So instead of changing the shape of RSDs through fine sediment deposition they instead have a softening effect on the sidewalls of the RSDs and can slightly alter the internal geometry of the RSD (Cacchione et al. 1987; Seafloor Mapping Lab at CSUMB: SFML Data Library, 2011).

However, RSDs have also been reported in areas without strong cross-shore currents, exposed outcrops or features that could redirect alongshore currents (Goff et al., 2005; Gutierrez et al., 2005). These subsequent findings have led to a shift away from the original hypothesis that sea floor geomorphology alone creates a "forced template" of where RSDs will form (Coco et al., 2007). Instead, others have proposed that bedform features self-organize through positive feedback mechanisms caused by local interactions between sediment and hydrodynamics. Studies have shown that increased wave energy and current velocities, like those created in high energy environments or during storm events, can be more conducive to RSD creation and perpetuation (Cacchione et al., 1984; Bellec et al., 2010; Storlazzi and Jaffe, 2002). It is therefore plausible that RSD abundance could be positively correlated with wave energy gradients, such as the latitudinal wave energy gradient along the California coast (Blanchette et al., 2006).

Murray and Thieler (2004) used an exploratory model to demonstrate that RSDs can arise from interactions between waves, currents, and bed composition, and thus independent of proximity to local topographic features, i.e., bedrock substrate, as originally suggested by Cacchione et al. (1984). They found that a turbulent event on a poorly sorted seabed could lead to selective concentration of coarser-grained sediment and form a domain with increased bed roughness relative to surrounding sediment. This increased roughness led to higher near-bed turbulence and to the advection of fine-grained sediment by currents, establishing a positive-feedback system that resulted in modeled bedforms very similar to those found in RSDs.

Despite this de-emphasized role of sea-floor structure in the formation of RSDs, bathymetry and geology may still promote and reinforce self-organization of these distinctive features. As waves shoal on the inner shelf, wave/seabed interactions (e.g., scattering, refraction, and bottom friction) increase (Shemdin et al., 1978). Additionally, bathymetric features such as banks, canyons, sand bars, and bedrock outcrops may significantly alter these interactions, and the width and slope of the shelf can cause significant wave energy loss (Putnam and Johnson, 1949). Shadowing caused by headlands and offshore islands, and the general aspect of the shelf, may also affect the exposure of the seabed to waves (Beyene and Wilson, 2007). The formation of RSDs could also be promoted by the presence of relict sediment deposits and other sedimentary facies by providing the coarser-grained sediment necessary to initiate self-organization (Browder and McNinch, 2006).

To date, our understanding of the patterns and processes associated with RSD formation and distribution have come from these local, site-specific studies conducted at the scale of kilometers. Now, with the recent completion of the California Seafloor Mapping Program (CSMP) providing comprehensive high-resolution multibeam bathymetry data along the State's entire 1200 km coast out to 3 nm and thus a majority of the inner continental shelf we have the ability to analyze region-wide data. Therefore the main goal of this study was to determine the extent to which the patterns and processes inferred from local RSD studies are supported by the spatial distribution of an entire population of RSDs at the regional scale.

A secondary goal was to assess the relative abundance of RSDs as an ecologically distinct *habitat* type compared to bedrock and non-RSD sediment habitats. Although RSDs have not been specifically addressed as a distinct benthic habitat in the ecological literature, many studies have shown that interactions of sediment grain size, bedforms, depth, and local hydrodynamics can profoundly influence the distribution and abundance of benthic species and community structure (Snelgrove et al., 1994; Ellis et al., 2000; Gray, 2002; Van Hoey et al., 2003; Lindholm et al., 2004; Brown and Collier, 2008). Moreover, in a companion study, Hallenbeck et al. (2012) found that

epibenthic communities inside RSDs in Monterey Bay, California were significantly more depauperate and less diverse than those of surrounding fine-grained substrate, but that young-of-the-year rockfishes (*Sebastes* spp.) and small flatfishes were strongly associated with RSDs. If these biotic differences are characteristic of RSDs, then the relative abundance and distribution of RSD substrate could have profound implications for benthic ecology, ecosystem based management, and marine spatial planning, particularly the design and monitoring of marine protected areas (MPAs).

Our objective for achieving the secondary goal of this study pertaining to the potential importance of RSDs in marine spatial planning and ecosystem based management was to evaluate how well the 68 individual MPAs within California's state-wide MPA network that fall within the geographic range of this study collectively represent regional percentages of bedrock, non-RSD sediment, and RSD substrate within California's four Marine Life Protection Act (MLPA) regions (Fig. 2).

From these goals, the following six predictions were made regarding the relative abundance of RSDs and where they are likely to form based on previous studies (Blanchette et al., 2006; Cacchione et al., 1984; Garrison, 2009; Green et al., 2004):

(1) The great majority of RSD substrate falls within the 20–80 m isobaths (Cacchione et al., 1984; Garrison, 2009; Molnia et al., 1983).
(2) Percent cover of RSD substrate increases with proximity to bedrock reefs (Cacchione et al., 1984).
(3) Percent cover of RSD substrate differs with latitude due to the wave energy gradient along the California coast, specifically North and South of Point Conception (Blanchette et al., 2006).
(4) RSD morphology is predominately elongate and shore normal (Cacchione et al., 1984; Green et al., 2004).
(5) Percent cover of RSD substrate differs with the geomorphology of the continental shelf including shelf width and proximity to headlands (Short, 1996).
(6) The proportion of RSD area inside of California's MPAs is not representative of the regional proportion of RSD area.

To evaluate these predictions, geospatial tools were developed to identify and classify RSD features in the CSMP digital elevation models (DEMs). The resulting RSD classification was then used to analyze the spatial distribution and relative abundance of RSDs on the California continental shelf compared to previously classified bedrock and sediment substrate coverages (Seafloor Mapping Lab (SFML) at California State University Monterey Bay (CSUMB): SFML Online Data Library).

2. Regional setting

California's exposed 1200 km long, wave-dominated coastline has a wide diversity of geomorphic features and oceanographic conditions. This variation makes the coast an ideal laboratory for assessing the relative importance of the various environmental factors thought to be associated with the occurrence and spatial distribution of RSDs on the continental shelf (Fig. 2). California's continental shelf is relatively narrow and steep, varying from 1 km to 46 km in width out to approximately the 130 m isobath. California's inner shelf is largely sediment deficient, with frequently exposed bedrock ridges, incised paleo-stream channels, and submarine canyons (Anima et al., 2002).

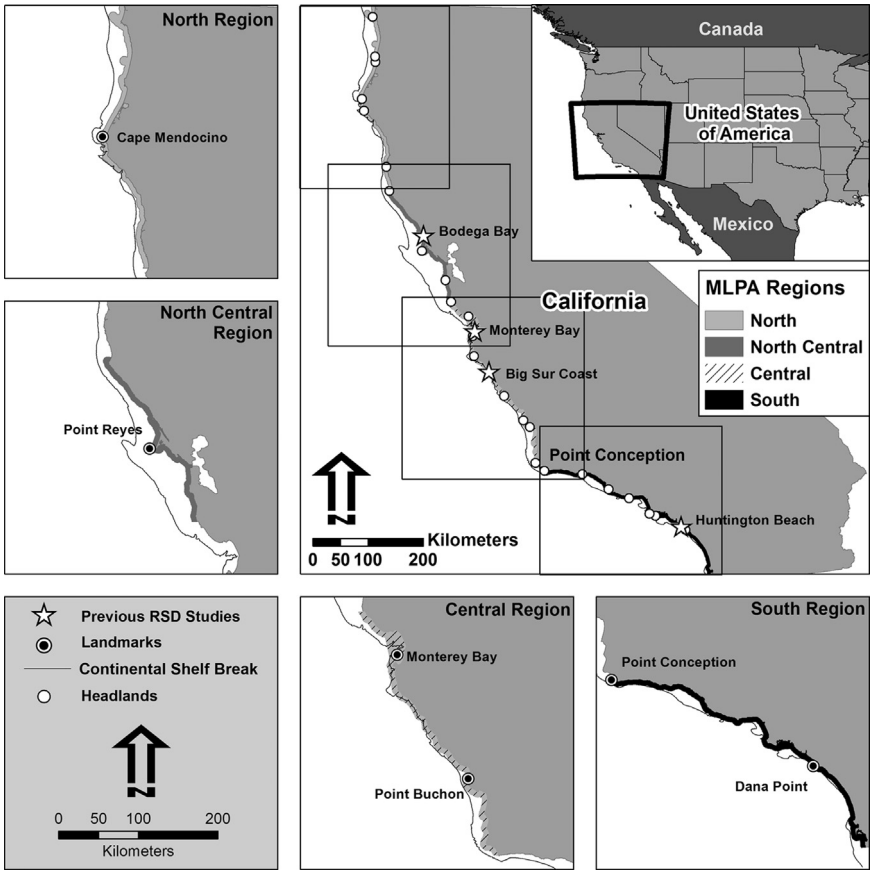

Fig. 2. Map of California's four MLPA regions. Stars indicate the approximate location of previous, localized RSD studies in California referenced in the text. Width of the regional outlines shown represents the 3 nm limit of state waters and the extent of the CSMP data used in the analysis. White circles denote the headlands used for analysis. The thin black line marks the location of the California continental shelf break, which generally follows the 130 m isobath.

During winter months, northwest deep-water waves from storms in the North Pacific impact California, while in the summer months longer period southwest swell arrives from storms in the Southern Ocean (Wingfield and Storlazzi, 2007). A positive south-to-north wave energy gradient exists along the coast (Bromirski et al., 2005), with Point Conception being a major transition point for shoreline morphology as well as oceanographic conditions such as dominant current and wave direction between southern and central California (Beyene and Wilson, 2007).

North of Point Conception the shoreline aspect is predominantly west-southwest, and the dominant California Current flows southward from the North Pacific Gyre. Subtidal flow is driven primarily by alongshore wind stress and a pressure gradient of equal, but opposing forces (Lentz, 1994). Currents on the inner shelf are weaker than generally predicted by models, possibly due to drag caused by the presence of large rock outcrops (Lentz, 1994). Near surface flow is generally offshore and weaker than bottom transport flow (Lentz, 1994), which even at depths of 200 m can produce bed shear stress capable of moving sand and sediment (Cacchione and Drake, 1990). South of Point Conception is a relatively protected area with weak wind driven currents and influences (Hickey, 1993) and a south-southwest shoreline aspect. Nearshore wave energy is significantly lower south of Point Conception due to this change in shore aspect and to shadowing caused by prominent offshore bathymetric features and islands (Beyene and Wilson, 2007). The complex circulation in the south is dominated by the Davidson Current, which runs northward from Baja California (Reid and Schwartzlose, 1962), the Eastern Bound Current and the California Current (Hickey, 1993). Additionally, the regional flow varies greatly with depth due to changes in channel width, and this stratification causes a strong vertical shear in currents (Hickey, 1993).

Previous descriptions of RSDs in California have come from the vicinities of Bodega Bay, Monterey Bay, Big Sur Coast, and Huntington Beach (Fig. 2), where a variety of different RSD formations and environmental conditions in which RSDs persisted over time were found (Cacchione et al., 1984, 1987; Cacchione and Drake, 1990; Hunter et al., 1988; Mariant, 1993; Eittreim et al., 2001; Ferrini and Flood, 2005; Phillips, 2007). The work presented here covers the entire California coast as far south as Dana Point, beyond which there is a lack of continuous high resolution bathymetric data of sufficient quality for detailed landscape analysis (Fig. 2). This study area was then subdivided for regional analyses and latitudinal comparisons into the four coastal regions designated by the MLPA: North Coast region (California/Oregon border to Alder Creek near Point Arena in Mendocino County), North Central Coast region (Alder Creek, near Point Arena, to Pigeon Point in San Mateo County), Central Coast region (Pigeon Point to Point Conception), South Coast region (Point Conception to the California/Mexico border), hereafter referred to as North region, North Central region, Central region, South region (Fig. 2). The individual MPAs within each region had been selected through the MLPA process with the intent that their collective substrate composition would be representative of the entire region. The habitat classification criteria used during the MPA design process consisted of two basic physical properties: depth zone (0–30 m, 30–100 m, 100–200 m, and >200 m) and substrate type (bedrock reef, soft-sediment), and did not include RSDs or other distinct sedimentary substrates (California Department of Fish and Game, 2008a, 2008b).

3. Methods

The CSMP data set is composed of 171 data blocks each covering approximately 5 km of the coast. The CSMP data products for each block include bathymetric digital elevation models (DEMs) and acoustic backscatter mosaics for areas within the California continental shelf depth range (<130 m isobath). Also included are shaded relief, slope, rugosity, and substrate classification raster grids derived from the DEMs. These products reveal the geomorphology of the sea floor including the depressions, bedforms and sharply delineated edges characteristic of RSDs (Fig. 1a). The backscatter imagery, which is proportional to sea floor acoustic reflectivity (higher substrate density and rougher texture yield stronger acoustic returns), is a useful aid in visually delineating the boundaries of RSDs due to the features' coarser-grained sediment reflecting stronger acoustic returns than the surrounding finer-grained sediment plains (Soulsby et al., 2012, Fig. 1b).

3.1. Auto-classification of RSD substrate

All geospatial analyses and classification of RSDs were conducted using ArcGIS software (ESRI, 2009) (see Table 1 for summary of all methods in Sections 3.1–3.5). To detect RSDs, we used a Topographic Position Index (TPI) algorithm that calculated the relative elevation of every point in the DEM compared to a defined neighborhood (Weiss, 2001), enabling accurate delineation of the distinct RSD boundaries. The multiple reclassification process created a binary raster with two exclusive values, one for RSD and one for everything else (non-RSD sediment and rock). The RSD raster data were visually compared to the TPI, DEM, and acoustic backscatter data and manually corrected in areas that were missed or misclassified. RSDs smaller than 100 m^2 were excluded from the classification to reduce errors attributable to fine-scale irregularities in the DEMs due to vessel motion and sonar processing artifacts, as well as disproportionately large edge effect associated with autoclassification of smaller features. The accuracy of the automated RSD classification was evaluated by running a single blind accuracy assessment tested using Cohen's Kappa inter-raster agreement test (Cohen, 1960).

The RSD raster data were merged with the original CSMP binary substrate raster data, which were previously classified into areas of “rough” and “smooth” topography. These “rough” and “smooth” classifications were used in the CSMP as proxies for defining rock and soft sediment substrates. The final combined product was a habitat raster classified into the three substrates of interest: rock, RSD, and non-RSD sediment. The binary raster was converted to a vector data set of polygons representing each individual RSD used to compare RSD size frequency distributions by region and depth.

A shelf raster was created to delineate the continental shelf and the continental slope. The criteria for the initial autoclassification of the location of the shelf break were chosen based on published studies placing the shelf break in California between 90 m and 200 m, and the mid-shelf break between 60 m and 90 m (Winant et al., 1987; Puig et al., 2003). The accuracy of the shelf break autoclassification results was then visually assessed and manually adjusted in areas of misclassification. Once designated (Fig. 2), the shelf break was used to further classify the substrate raster into shelf and slope areas. The following analyses of RSD distribution were confined to the continental shelf because few RSD features were observed deeper than this defined shelf break in the CSMP data set and they would presumably undergo different mechanisms of creation and perpetuation than those on the shelf.

3.2. Grain size comparison

To verify that the RSDs identified in this study contained coarse-grained sediment consistent with the descriptions of RSDs reported in previous studies, data from the usSEABED database (Reid et al., 2006) were used to compare sediment grain size for

Table 1
Summary of methods, including data used, processes performed, products created, and tests run using that product.

Section	Data used	Methods used	Products created	Analysis performed
3.1. Auto-classification of RSD substrate				
TPI and RSD auto classification	CSMP bathy DEM	An annulus with an inner radius of 30 m and outer radius of 35 m, classified all areas with a TPI value less than or equal to −11 as "RSD", and other areas as "other". The data were repeatedly reclassified such that any "other" data within a 2 pixel radius of "RSD" pixels, with a TPI value >= −8, were designated as "RSD" to enhance boundary detection.	TPI layer, RSD binary raster	NA
Data merging	RSD layer, CSMP substrate raster	Raster calculator to merge two raters in ArcGIS spatial analyst tool	3-habitat combo raster	NA
Conversion to vector polygon	3-habitat combo layer	Conversion tool-"Raster to Polygon" in ArcGIS	RSD only vector polygon	NA
Defining shelf break	CSMP bathy DEM, CSMP slope raster	The data were visually analyzed to create a best-fit algorithm that classified shelf break if its depth was in a range of 60 m to 130 m and a slope greater than 15°. The accuracy of the autoclassification results was visually assessed and manually adjusted in areas of misclassification.	Shelf and slope raster	NA
3.2. Grain size comparison				
	usSEABED data, MLPA region shapefile	Point shape file with grain size attribute created from GPS coordinates samples. Grain size compared to RSD binary raster classification for North Central, Central, and South MLPA regions	NA	one-way ANOVA with TukeyHSD multiple comparisons
3.3. RSD classification categories				
Rock only layer	CSMP 2-habitat raster	a "rock only" raster was created and "grown" around the rock clusters using a Euclidian distance of 25 m, converted to a polygon using Conversion Tool-"Raster to Polygon" in ArcGIS	Bedrock reef layer, bedrock reef vector polygon	
Assigning classification attributes	RSD vector polygon layer, CSMP bathy DEM, bedrock reef vector polygon	Select by Attribute and Select by Location Tools in ArcGIS were used to determine the depth of each RSD's centroid, total area, and if it inteceted with the bedrock reef polygon layer	RSD vector polygon with multiple class attributes, attribute table	Number and area of each class summed
Assigning morphology attributes	RSD vector polygon layer, CSMP bathy DEM, simplified coastline polygon	A simplified polygon shapefile was created using the Bounding Containers tool (Patterson, 2010), length, width, area, and aspect of each of the simplified RSD polygons were calculated. RSD aspect compared to the aspect of the simplified coastline polygon	RSD vector polygon with multiple class and morphology attributes, attribute table	Number and area of each morphology type summed
3.4. RSD distribution analyses				
Depth	CSMP bathy DEM, RSD raster	Bathymetry DEMs were converted into 1 m depth intervals and the area of RSD and other substrate types were calculated for each 1 m interval	% cover by depth output table	
Proximity to rock	Bedrock reef layer, RSD raster	Euclidian distance from the nearest bedrock reef was calculated in 50 m intervals. The area of each substrate type was calculated in each 50 m interval up to a 5 km maximum distance	% cover by proximity to rock output table	
Latitudinal gradient	USACE W.I.S. hindcast station data, NOAA state water boundary polygon	Buoy station data were grouped and averaged in blocks of four alongshore segments spanning 1.5 degrees of latitude (167 km). Each composite is an alongshore mean of hourly observations of wave height, period, and direction.	10 km UTM block latitude shapefile, output table	Spearman's non-parametric correlation test
Shelf width	Shelf raster, 10 km latitude shapefile	Average continental shelf width was determined for each of the previously created 10 km latitudinal bands, constrained to areas shallower than 80 m to standardize the result.	output table	Square root transformation, Pearson's correlation test
Headlands	RSD raster, lighthouse coordinates data	Created "headland" point shapefile using GPS coordinates of 25 known lighthouses, then used the Buffer Tool to create the various headland buffers.	1, 5, 10, 15, 20, and 25 km headland buffers	ANOVA, T-test
3.5. RSD distribution within marine protected areas				
	MLPA region shapefile, MPA boundary shapefile, 3 habitat combo raster, bathymetry DEM	Calculated percent area of each substrate type using the MPA boundary shapefile. Stratified for regional substrate comparisons within MLPA depth zones (0–30 m, 30–100 m and 100–200 m).	Output table	T-test to compare percent cover inside MPA and overall MLPA region percent cover

samples collected inside and outside of the RSD features delineated in the substrate raster within each of the MLPA regions. Because no samples in the sediment data base coincided with RSDs in the North region where usSEABED samples were scarce, the analysis was necessarily restricted to the North Central, Central, and South regions. A one-way ANOVA with Tukey HSD multiple comparisons was used to detect significant differences in the mean grain size between RSD and non-RSD areas in these three regions.

3.3. RSD classification categories

Previous studies of RSDs in New Zealand and on both coasts of North America have sought to classify RSDs into categories based on morphology, depth, and distance from shore (Cacchione et al., 1984; Ferrini and Flood, 2005; Green et al., 2004). Building on the classification descriptions from Green et al. (2004), five different RSD classes were identified based on depth, proximity to bedrock reef, and size (Table 2). These classes were designated as: inshore,

Table 2
Summary of characteristics used to classify RSDs into categories based on distance from shore, association with bedrock reef, size, shape and orientation to shore.

Category	Specifications	Justification
Inshore	Centroid less than 20 m depth	RSD percent cover reaches its maximum at a depth deeper than 20 m (Cacchione et al., 1984)
Offshore	Centroid greater than 20 m depth	
Inshore rock-associated	Centroid less than 20 m depth, touching bedrock reef outcrop	
Offshore rock-associated	Centroid greater than 20 m depth, touching bedrock reef outcrop	
Mega	Total area greater than 10 km², making them the dominant sediment type along that portion of the coast.	Based on a natural break in the size distribution of individual RSDs that occurred between 7 km² and 10 km²
Elongate	Length to width ratio greater than or equal to 3:1 was classified as elongate.	Ferrini and Flood (2005), confirmed by natural break point in the length/width ratio distribution observed in the data
Shore Parallel	Orientation to the shore of 0° to 30°	
Shore normal	Orientation to the shore of 31° to 60°	
Oblique	Orientation to the shore of 61° to 90°	

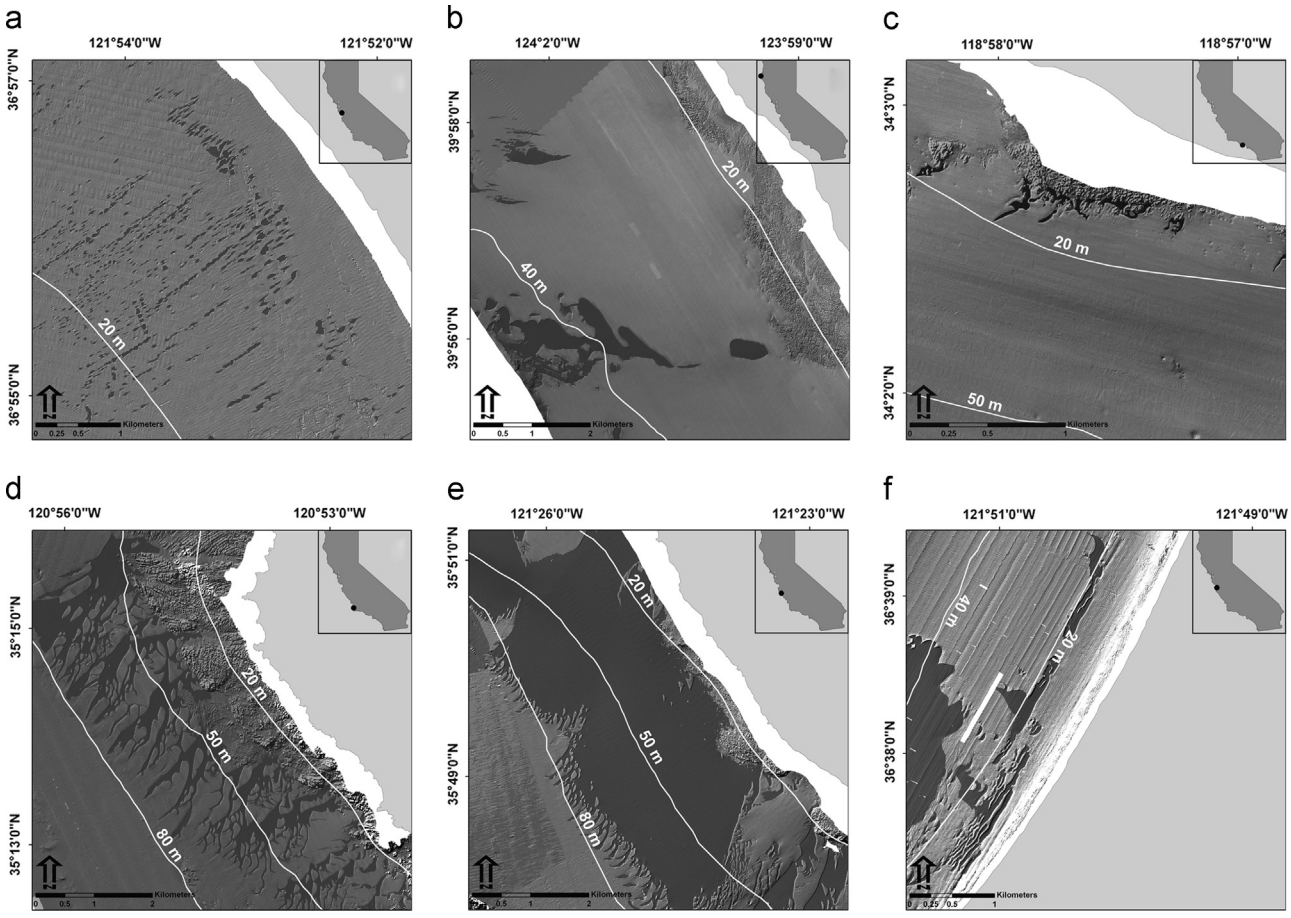

Fig. 3. Shaded relief bathymetry with RSD features darkened to illustrate examples of five RSD classification categories found on the California continental shelf based on depth, proximity to bedrock reef and size. (a) Inshore (< 20 m depth) RSDs. (b) Offshore (> 20 m depth) RSDs. (c) Inshore rock-associated RSDs. (d) Offshore rock-associated RSDs. (e) Mega RSDs. Examples of the three different RSD classes based on morphological characteristics are shore-normal and elongate (a), shore-oblique (b), and shore-parallel and elongate (f). Location of each panel is represented by the black dot on the California map in the upper right corner.

offshore, inshore rock-associated, offshore rock-associated, and "mega" (Fig. 3). Mega RSDs were originally classified, but were not used in any analyses due to their size ($>10\ km^2$), making them the dominant sediment type in the area, and potentially not subject to the same processes of formation and perpetuation. RSDs were then subcategorized by morphology and orientation to shore as: shore normal, shore parallel, oblique, and elongate or not (Fig. 3).

To determine the spatial distribution patterns, each RSD polygon was assigned to one of the four specific classes. The quantity and area of each class was summed for the entire mapped area of the California continental shelf and each of the MLPA regions. In addition to these classes, each RSD was also evaluated in terms of its morphology and orientation to shore (aspect) (Tables 1 and 2).

3.4. RSD distribution analysis

The percent cover for each of the substrate types (rock, RSD, and non-RSD sediment) was calculated for the entire shelf within state waters. Tests of statistical significance were only run on the latitude, shelf width, and headland analyses because all other analyses (below) used the entire population of RSDs and shelf substrate types to assess the patterns of distribution and abundance.

To quantify variation in substrate percent coverage relative to depth, the bathymetry DEMs were converted into 1 m depth intervals and the area of RSD and other substrate types were calculated for each 1 m interval for each region. To determine the substrate percent cover relative to proximity to bedrock substrate, the Euclidian distance from the nearest bedrock reef was calculated in 50 m intervals. The area of each substrate type was calculated in each 50 m interval up to a 5 km maximum distance, excluding the first 50 m interval, which was excluded to remove any sedimentary patches completely enclosed within areas of bedrock. Small, isolated bedrock outcrops smaller than $10{,}000\ m^2$ were also considered artifacts and excluded from the analysis.

To test for a relationship between wave energy and RSD substrate cover, size, morphology, and proximity to bedrock substrate, latitudinal gradient analyses were performed on RSD distribution and wave data along the entire coast. To test for the presence of a latitudinal gradient in RSD percent cover, the area of each substrate type was quantified within 10 km intervals. Hourly composites from 25 U.S. Army Corps of Engineers Wave Information Studies (USACE, 2012) hindcast stations for the time period 1981–2004 were used to quantify the latitudinal distribution of wave height, wave direction, and frequency along the coast. A Spearman's non-parametric correlation test was run to determine the strength and significance of the associations between latitude and RSD percent cover, RSD size, RSD morphology, and RSD proximity to rock.

To test for a relationship between continental shelf width and RSD substrate cover, the average continental shelf width was determined for each of the previously created 10 km latitudinal bands. RSD percent cover was calculated from the substrate rasters for each of these bands. However, because the vast majority of RSD substrate observed along the entire coast was found inshore of the 80 m isobath regardless of shelf width, the percent RSD substrate cover calculation was constrained to areas shallower than 80 m to standardize the results. The RSD percent cover data were then square root transformed and a Pearson's correlation test was run to determine if RSD percent cover was correlated with the shelf width values. Additionally, an ANOVA and Tukey HSD post hoc were run to test for significant differences in the shelf widths of the four MLPA regions.

To test for a relationship between RSD and proximity to headlands, major headlands along the California coast were selected by proxy using the known coordinates for lighthouses. Twenty-four different headlands were selected and examined to ensure they captured a range of headland features that varied in shape, size, and morphology (Fig. 2). An ANOVA tested for any significant difference between the headlands buffer sizes and a Student's T-test was run to detect any difference in the RSD percent coverage within the buffers and the total statewide RSD percent coverage.

3.5. RSD distribution within marine protected areas

Lastly, to assess the potential impact of incorporating RSD substrate maps into existing marine spatial planning programs, the accuracy of the established MPAs collectively capturing proportional amounts of rock, RSD, and non-RSD sediment substrate representative of the four MLPA regions was evaluated. The percent cover of all three substrate types in the four coastal regions was calculated, and the MPA boundary shapefiles were then used to calculate the percent cover of the substrates inside each MPA as well as the mean percent cover for all MPAs by region. To assess if the MPA network included a representative amount of each substrate, we calculated the total percent area of each substrate type inside all MPAs in a MLPA region and compared it to the overall percent cover for that region. These analyses were also stratified for regional substrate comparisons within each of the three relevant MLPA depth zones (0–30 m, 30–100 m and 100–200 m).

4. Results

4.1. Auto-classification of RSDs

Over 6000 individual RSDs larger than $100\ m^2$ were identified within the mapped area, ranging in size from $103\ m^2$ to $40\ km^2$ (RSDs $<100\ m^2$ were not classified). The accuracy assessment of the RSD classification and the inter-observer agreement showed that the classification of RSDs was accurate and repeatable. The Cohen's Kappa test for the comparison between the visual assessment and RSD classification showed a very good agreement of 98.9% between the two methods (KHAT = 0.919, $p < 0.00001$).

4.2. Grain-size comparison

The grain sizes of all usSEABED samples from sites classified as RSD substrate were significantly larger ($0.42\ mm \pm 0.26$,

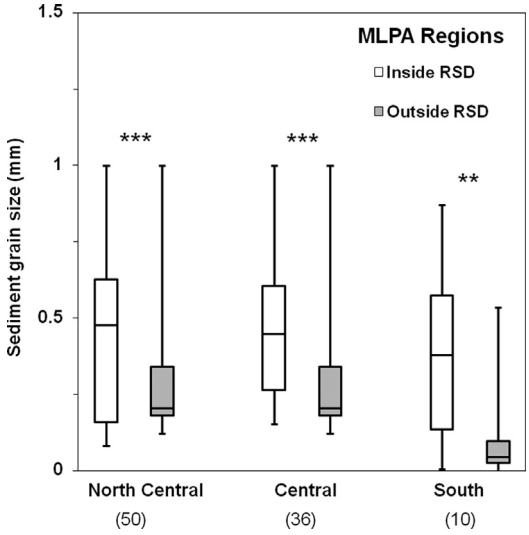

Fig. 4. Grain size (mm) of usSEABED sediment samples from locations identified as inside and outside of RSDs in the North Central, Central, and South MLPA regions. Whiskers represent maximum and minimum values, horizontal lines represent the mean, and boxes represent 1st and 3rd quartile. Sample sizes (number of paired points) are shown in parentheses. P-values represented by *=0.05, **=0.01, ***=0.001.

mean ± SE, $n=96$) than those for all selected samples from the non-RSD sediment areas across all regions where samples were available (0.24 mm ± 0.17, mean ± SE, $n=96$) ($F=12.49$, $df=7$, $p<0.005$). (Fig. 4). The differences in mean grain sizes found inside versus outside RSDs are comparable to those reported (0.28–0.78 mm) in other RSD studies along the California coast (Cacchione et al., 1984; Mariant, 1993; Phillips, 2007; Hallenbeck et al., 2012).

4.3. RSD morphology

The distribution and relative abundance of the five different categories of RSDs were not uniform along the coast (Fig. 5). The non rock-associated (inshore and offshore) RSDs were the most common form found in all four of the MLPA regions, accounting for 79% of all identified individual RSDs. However, these non-rock associated RSDs accounted for only 26.8% of total RSD substrate area identified on the California shelf. Conversely, rock-associated RSDs were far less abundant in number accounting for only 6.1% and 14.9% of all individual inshore and offshore RSDs respectively, but 1.9% and 71.3% of the total inshore and offshore RSD substrate area along the California coast.

North of Point Conception, rock-associated offshore RSD was the most abundant RSD class by area for all three MLPA regions, North, North Central and Central, representing 81%, 74% and 47% of all RSD substrate respectively. Rock-associated offshore RSDs were very rare in Southern California (3% of regional RSD quantity and 18% of total RSD area) (Fig. 5). This distribution is consistent with the abundance of bedrock reef substrate north and south of Point Conception, which is 10% and 1.5% respectively (Table 3). The density (number of individual RSDs per km^2) and the percent of non rock-associated RSDs on the shelf were both highest in the South region (Fig. 5). The density and percent cover on the shelf was low in all regions for the inshore rock-associated class (Fig. 5). The mean RSD sizes for each of these classes were significantly

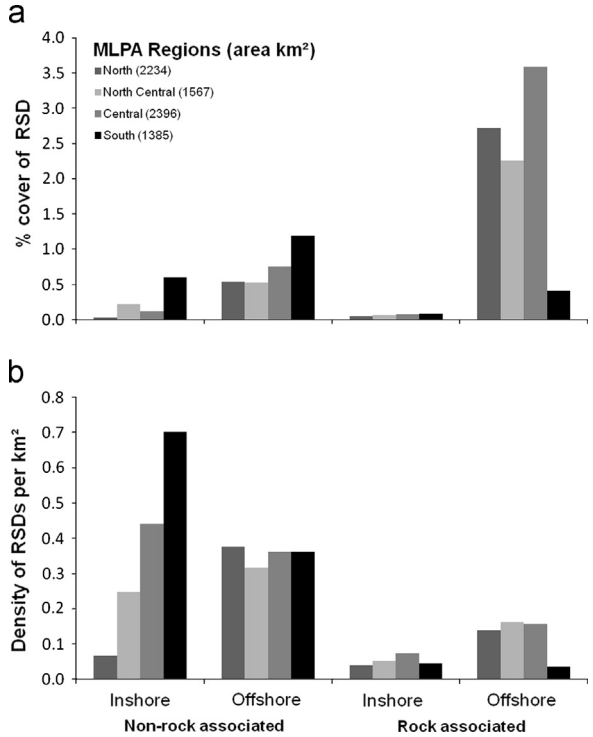

Fig. 5. Distribution of (a) percent cover of RSD substrate on the continental shelf and (b) density of RSDs (number per km²) by category (inshore versus offshore, and non-rock versus rock associated) throughout the four MLPA regions.

Table 3
Percent substrate coverage by depth zone for the entire coast (All) and the four MLPA regions, with values given for each region as well as the pooled values from all of the marine protected areas (MPA) within each region. Sediment substrate values represent all non-RSD sediment areas.

MLPA Regions			%Sediment		%RSD		%Rock	
	Depth	Total area (km²)	Region	MPA	Region	MPA	Region	MPA
All	0–30	2677.9	83.9	68.0	2.8	2.3	13.4	29.7
	31–100	4097.9	89.9	85.7	4.4	6.3	5.8	8.1
	100–200	251.2	99.2	98.9	0.1	0.2	0.8	0.9
	Total	7027.0	88.0	81.4	3.6	4.9	8.4	13.7
North	0–30	686.1	86.8	88.9	1.3	0.3	11.9	10.9
	31–100	1122.7	88.2	85.8	5.2	3.5	6.6	10.7
	100–200	129.9	99.4	97.8	0.0	0.0	0.6	2.2
	Total	1938.7	88.3	87.4	3.5	2.4	8.1	10.2
North Central	0–30	500.2	78.5	50.6	2.5	2.1	19.0	47.2
	31–100	854.7	90.1	84.5	3.6	6.4	6.3	9.2
	100–200	0.0	0.0	0.0	0.0	0.0	0.0	0.0
	Total	1354.8	85.6	77.8	3.1	5.5	11.3	16.7
Central	0–30	586.1	78.3	68.4	3.0	2.2	18.7	29.4
	31–100	1308.9	87.4	80.8	5.8	9.3	6.8	9.9
	100–200	109.5	98.9	98.6	0.1	0.3	1.0	1.1
	Total	2004.6	85.1	78.1	4.6	6.1	10.2	15.8
South	0–30	547.7	98.4	91.0	4.8	3.0	2.2	5.9
	31–100	580.7	100.0	97.9	0.7	0.1	0.9	1.9
	100–200	9.9	95.8	100.0	0.0	0.0	0.0	0.1
	Total	1138.4	88.0	96.3	2.6	0.9	1.5	2.8

Table 4
Distribution of RSDs by orientation throughout the four MLPA regions.

Region	Regional RSD abundance by type				
	Orientation	**Non rock-associated**		**Rock-associated**	
		Inshore (%)	Offshore (%)	Inshore (%)	Offshore (%)
North ($n=1390$)	Shore normal	65.6	57.6	37.5	49.4
	Shore parallel	18.5	16.0	27.3	14.7
	Oblique	15.9	26.5	35.2	35.9
North Central ($n=1221$)	Shore normal	57.8	61.2	36.6	53.5
	Shore parallel	16.2	10.5	22.0	13.4
	Oblique	26.0	28.3	41.5	33.1
Central ($n=2485$)	Shore normal	78.9	56.8	40.4	44.4
	Shore parallel	9.2	11.9	28.1	24.6
	Oblique	11.9	31.3	31.5	31.0
South ($n=1587$)	Shore normal	48.3	62.2	41.3	41.2
	Shore parallel	16.1	8.2	27.0	27.5
	Oblique	35.6	29.7	31.7	31.4

different from each other ($F=3806.4$, $df=4$, $p<0.0002$) (ANOVA, $df=4$, $F=3806.4$, $p<0.0002$). The North region had the largest RSD mean size while the South had the smallest.

The statewide distribution of RSD morphological classes followed a similar pattern to those described in or predicted from earlier site-specific studies (e.g. Cacchione et al., 1984), as shown in Table 4. The majority (66%) of all RSDs found along the California coast were shore-normal and elongate in form

(Table 4 and Fig. 6). However, when separated by MLPA region, the North region had the highest percentage of shore-parallel RSDs (17%), the Central region had the highest percentage of shore-normal RSDs (63%), and the South contained the highest percentage of shore-oblique RSDs (34%).

When these morphological traits were combined with the five distributional classes the majority of all RSDs were elongate (52%) and shore normal (57%). The majority of both inshore (54%) and offshore (60%) RSDs were also elongate in shape. Conversely, the majority (68%) of the two rock-associated categories were not elongate in shape. The South had the highest density of non rock-associated RSDs and the lowest densities of the rock-associated classes (Fig. 5 and Table 4). The density of the offshore non rock-associated and the inshore rock-associated groups, however, was similar along the coast, and the North Central region had the highest density of offshore rock-associated RSDs (Fig. 5).

4.4. RSD distribution analysis

As predicted, RSDs proved to be a widespread and common substrate type along the California continental margin, comparable in abundance to that of bedrock reef substrate (Table 3). The percent cover analyses found that RSDs covered 3.6% (253 km^2) of the entire mapped shelf area, while bedrock reef substrate and non-RSD fine-grained sediment areas accounted for 8.4% (590 km^2) and 88% (6184 km^2), respectively. Large individual RSDs with an area greater than 1 km^2 accounted for the majority (67%) of RSD substrate, however, RSDs smaller than 1 km^2 comprised 99% of the total RSD population (Fig. 7). Although overall RSD percent cover was 2.5 times higher north of Point Conception than to the south, the total quantity of RSDs varied inversely with size class for both of these regions (Fig. 7). The overall density of smaller RSD features ($< 10^5$ m^2) was greater south of Point Conception, whereas the density of larger RSD's ($> 10^5$ m^2) was higher north of Point Conception (Fig. 7).

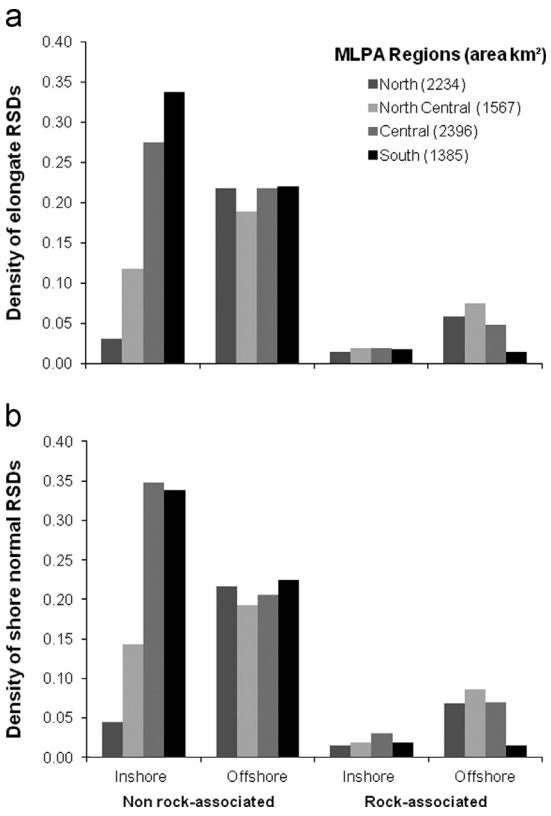

Fig. 6. Distribution by MLPA region of RSD density per km² based on morphological characteristics. (a) Distribution of elongate RSDs. (b) Distribution of shore-normal RSDs.

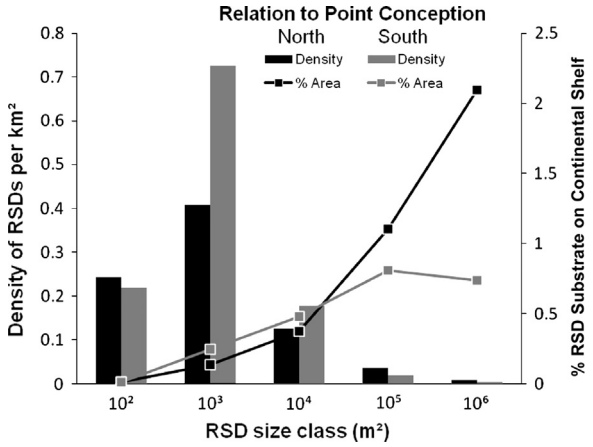

Fig. 7. Distribution of RSD density (bars) and percent of RSD substrate on the continental shelf (lines) by size class for the entire California coast north (black) and south (gray) of Point Conception. Size classes are represented on a log scale.

When tabulated by MLPA region (Table 3), the Central region had both the highest RSD coverage with 4.6%, and the South region the lowest (2.6%). The South region, however, contained nearly twice as much RSDs substrate compared to bedrock reef substrate, whereas all three regions north of Point Conception contained more rock than RSD substrate (Table 4).

4.4.1. RSD distribution by depth

The results for RSD percent cover with respect to depth are consistent with those from previous site-specific RSD studies (Cacchione et al., 1984; Green et al., 2004; Ferrini and Flood, 2005; Garnaud et al., 2005; Iacono and Guillen, 2008; Bellec et al., 2010). Here, 82.3% of RSDs identified occurred between the 20 m and 80 m isobaths with peak RSD percent cover occurred at a depth of 46 m (Fig. 8a). The results show 6.5% of RSD substrate was found in depths greater than 80 m, however all of these RSDs began in depths shallower than 80 m, and 11.2% was found in depths shallower than 20 m. The depth at which peak RSD cover occurred increased regionally along a south to north gradient (Fig. 8a). South of Point Conception, RSD percent cover was concentrated in depths less than 30 m with peak RSD cover at 22 m. In the three regions north of Pt Conception, the vast majority of RSD substrate occurred in depths greater than 30 m (Fig. 8a,b) and peak RSD percent cover occurred between 40 m and 60 m. The Central region percent cover peaked at 43 m, the North Central region peaked at 52 m and the North region RSD percent cover peaked at the greatest depth (57 m). The RSDs in the Central region occurred across the broadest depth range (1–110 m), with a mean depth of 57 m, and the south had the narrowest range of 1–55 m depth.

4.4.2. RSD variation with proximity to bedrock reef substrate

For the North, North Central, and Central regions, RSD percent cover increased with proximity to bedrock reef substrate, with the highest percent cover occurring within 100 m of bedrock reef (22.6%), and over 60.9% of all RSD substrate within 500 m of bedrock reef substrate (Fig. 9a). Approximately 12.7% of the sedimentary substrate was within 100 m of bedrock reef substrate, and 30% was within 500 m of bedrock reef substrate, signifying a disproportionately large percent of RSDs within 500 m of bedrock reefs. South of Point Conception, however, there was no detectable association of RSDs with bedrock reef substrate, until a spike in coverage at a distance of 4.6 km from bedrock reefs (Fig. 9b). This

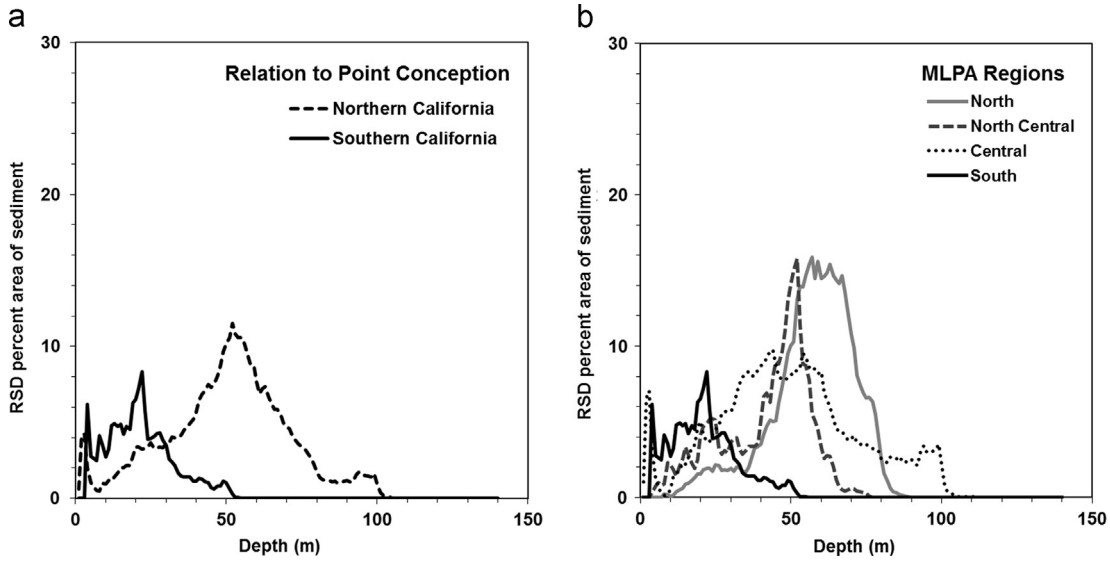

Fig. 8. (a) Overall RSD distribution by depth in northern and southern California, and (b) RSD distribution by depth by MLPA region.

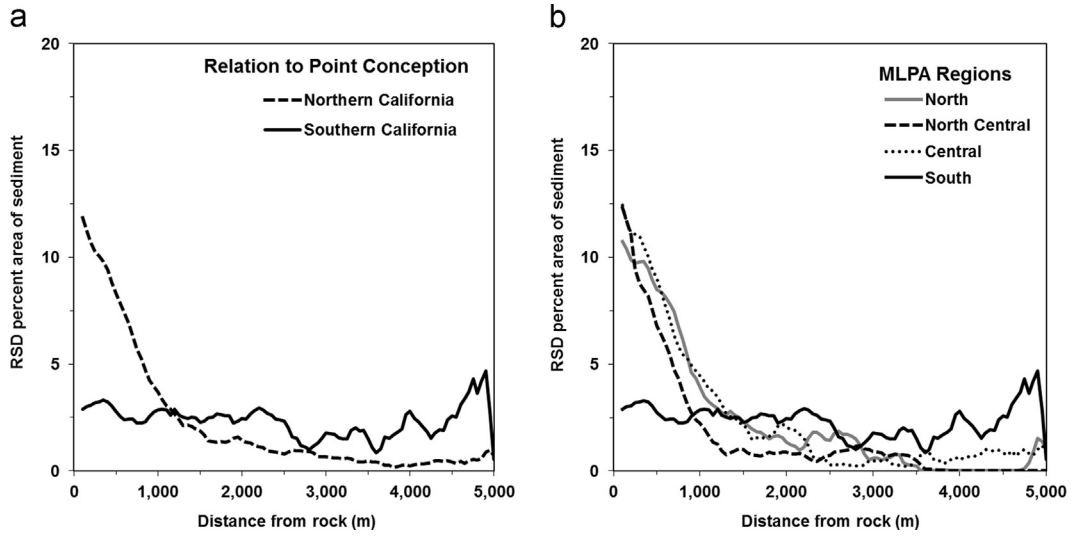

Fig. 9. (a) RSD % cover with respect to distance from rock for northern and southern California, and (b) the different MLPA regions.

difference could be related to bedrock reef substrate being five to seven times less common south of Point Conception than in the three regions to the north, and the South being the only region to have a higher percentage of RSD than bedrock reef substrate (Table 3). This pattern suggests that the overall relationship between the distribution of RSDs and proximity to bedrock reef substrate is uniform north of Point Conception, and that the difference south of Point Conception is likely due to the much lower cover of bedrock reef substrate.

4.4.3. Distribution by latitude

Results of a Spearman's non-parametric correlation test of latitude versus wave energy suggest that wave energy was positively correlated with latitude along California's coast ($r=0.778$, $p=0.008$). The results from the USACE hindcast data analysis show that there is also a consistent positive gradient in the percentage of waves higher than 6 m from south to north (Fig. 10). The results of the Spearman's non-parametric correlation test of latitude versus RSD percent cover found a weak but significant large-scale negative correlation between latitude and RSD percent cover ($r=-0.228$, $p=0.02$) for the entire California coast. North of Point Conception, RSD percent cover also displayed a weak but significant negative correlation with latitude ($r=-0.325$, $p=0.002$), but not to the south ($r=0.563$, $p=0.07$).

Additional correlation tests on latitude versus morphology and orientation showed that there was no correlation between offshore, and offshore rock-associated ($r=-0.183$, 0.018, and -0.099 respectively, $p>0.05$). There was a weak, but significant negative correlation between latitude and inshore rock-associated, oblique, shore parallel, shore normal, and elongate RSDs ($r=-0.276$, -0.284, and -0.277, -0.333, and -0.330 respectively, $p<0.05$). The inshore non rock-associated category had a moderate negative correlation with latitude ($r=-0.462$, $p<0.0005$).

4.4.4. Shelf characteristics: width and headlands

Results of the shelf width analysis showed that there was a weak, but significant, negative correlation between the percent cover of RSD substrate and shelf width (Pearson's correlation $r=-0.270$, $p=0.007$) (Fig. 11). There was also a significant difference in the shelf width between MLPA regions ($F=30.28$, $df=3$, $p<0.0005$). A post-hoc Tukey

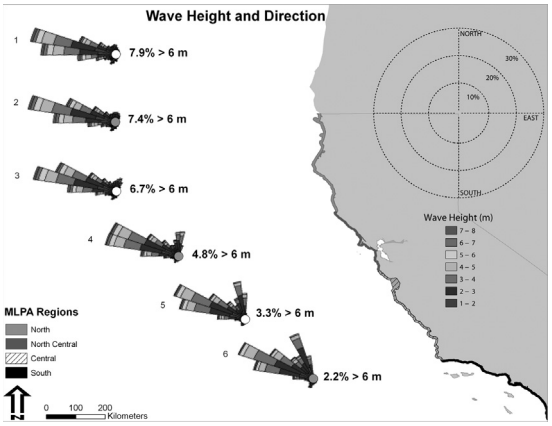

Fig. 10. Latitudinal offshore wave height gradient along California coast. Map of wave roses created from United States Army Corps of Engineers hindcast model data (USACE, 2012). Wave height is indicated with a grayscale ramp; wave direction by the azimuth of the "petals" of the wave rose in 10° increments, and percentage of waves by the radial length of the bands.

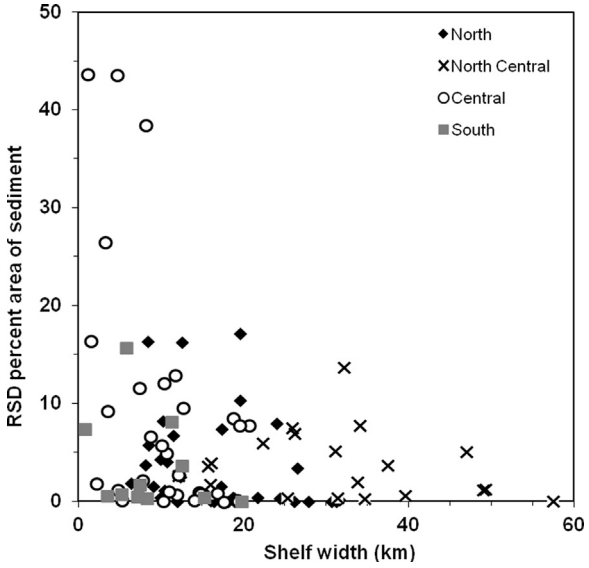

Fig. 11. Regional comparison of RSD percent area of sediment substrate inshore of the 80 m isobath calculated for each shore-normal, 10 km wide latitudinal strips plotted with respect to the continental shelf width for each strip.

test showed that there was a significant difference between all regions ($p < 0.02$), except the South and Central MLPA regions.

In some areas, such as the Big Sur coast in the Central MLPA region where the continental shelf is narrow (mean width 10.8 km ± 5.8 km SD), the RSD % area was high across the entire shelf (Fig. 11). In places where the shelf is wider, such as south of San Francisco Bay in the North Central region (mean width 31.1 km ± 12.6 km SD), RSD % cover was lower. These patterns, however, did not hold true south of Point Conception, where RSD % area remained low regardless of the Southern region's generally narrow shelf (mean width 8.9 km ± 5.5 km SD).

The proximity to headlands appeared to have no influence on the distribution and abundance of RSD substrate. The analysis found no significant association between RSD substrate coverage and distance from headlands ($F=0.0155$, $df=141$, $p=0.901$).

4.5. RSD distribution within marine protected areas

Comparison of the substrate analysis results (Table 3) confirmed that State-wide, the mean percent cover of RSD and non-RSD sediment substrate generally matched the proportions of these substrates collectively captured by the entire MPA network. State-wide bedrock substrate, however, was found to be over-represented by the MPA network across all depth zones by a factor of 1.6, and a factor of 2.2 within the shallow (< 20 m) depth zone. Regionally, RSD and non-RSD sediment substrate coverages were all generally close to those found within the MPA network, with the exception of the South region, where the overall regional RSD cover was nearly three times greater than within the MPA network. Another disparity in MPA/Regional RSD cover was in the shallow zone (0–20 m) of the North region, where regional RSD coverage was five times greater than within the MPAs.

5. Discussion

The results of this study support four out of the six predictions that were made on the distribution and abundance of rippled scour depressions. As predicted, the majority of RSD substrate occurred between the 20 m and 80 m isobaths (Cacchione et al., 1984; Garrison, 2009; Molnia et al., 1983). It was also hypothesized that RSD percent cover would decrease with depth given the negative relationship between depth and wave interactions with the sea floor (Storlazzi and Reid, 2010); however, we found that percent cover increased with depth out to approximately the 50 m isobath, then decreased to the 80 m isobath beyond which RSD substrate was rare. At depths greater than 80 m, waves may not have sufficient interaction with the bottom to create the conditions needed for RSD ripple formation, but as waves move into shallower depths, the speed of near-bed wave orbital motions increases, as does RSD percent cover (Bellec et al., 2010). However, at depths shallower than 50 m, conditions appear to again become sub-optimal for RSD formation or maintenance as RSD percent cover begins to decrease. This pattern may either be due to the speed of the oscillatory wave motions becoming too great for RSD formation or due to wave energy dissipation caused by bottom friction (Evans, 1942).

Secondly, we predicted, and found, that RSD substrate percent cover would increase with proximity to rock. Cacchione et al. (1984) first proposed that bedrock reef substrate could be a major contributing factor in the formation of RSDs by channeling and focusing bottom currents to create localized areas of higher current flow leading to the formation of RSDs. Studies in Australia (Field and Roy, 1984) and Canada (Hequette and Hill, 1993) described similar focusing of bottom currents in bedrock reef channels. The coarse-grained relict sediment deposits associated with paleo-stream channels may also contribute to the initial formation of RSDs (Browder and McNinch, 2006). RSDs, however, have also been observed in areas with no exposed bedrock reef especially in bays, shallow waters, or wide sandy margins characteristic of Southern California and along the East Coast of the United States (Goff et al., 2005). The presence of RSDs in such areas suggests that the process of RSD formation can occur in the absence of bedrock reef substrate, although it may favor their formation. These findings indicate that a different set of RSD formation processes may be more dominant in Southern California where there is a higher percentage of sandy shoreline, less abundant bedrock reef substrate (Table 3), and generally smaller (Fig. 7) and shallower RSDs (Fig. 8). Conversely, RSDs found associated with rock outcrops made up 80% of all RSD substrate on the California shelf. These rock-associated RSDs were also observed to be generally larger in size than the RSDs found in sandy areas. Thus, while the presence of bedrock reef substrate is not always necessary for RSD occurrence, it may play an important role in the formation and persistence of RSDs and in the development of large expanses of RSD substrate (e.g., mega RSDs).

Despite the positive correlation found between wave energy and latitude, there was a negative correlation between RSDs and latitude (prediction 3). This result suggests that finer scale spatial and temporal sampling and modeling of wave energy will be required to understand latitudinal variation in RSD distribution.

The predictions about RSD morphology (prediction 4) based on Cacchione et al., 1984 and Green et al., 2004 supported their findings. We found that 66% of all RSDs along the California coast were elongate in shape and shore normal in orientation. As for the predictions based on the shelf geomorphology (prediction 5) we found mixed results. We did find a significant negative correlation between RSD cover and shelf width, but no association between headlands and RSD cover. This latter result may be due to the very wide size range of the relatively small number of headlands included in the analysis. Features such as Cape Mendocino and Point Conception may be too large to influence local distribution of RSDs, and a headland analysis restricted to smaller features may prove more insightful.

The results from the MPA analysis (prediction 6) are contrary to our hypothesis that because RSD substrate was not taken into consideration when the MPA network was designed, it would not be accurately captured by the MPAs for any of the regions. Instead, we found that the MPA network represents the regional abundance of RSDs quite well, with regional versus MPA proportions generally within one or two percentage points of each other (Table 3). Conversely, mean bedrock reef substrate, which was considered during the design of the MPA network, was actually higher than the regional percent cover in all four MLPA regions, and was consistently over-represented in all but two of the 12 regional depth zones. Therefore, the existing MPA network more accurately reflects the regional abundance of RSD substrate than bedrock reef substrate. Moreover, several individual MPAs contained RSD substrate cover equal to or exceeding that of their region as well as that of bedrock reef substrate. For example in the Point Buchon MPA (Central region, Fig. 2), RSD and bedrock reef substrates each represent 26% of the MPA. The large amount of the RSD substrate documented here for the California shelf and MPA network supports the addition of a third substrate type to the MLPA classification scheme to more accurately represent ecologically distinct benthic habitats.

Mega RSDs (which were left out of the general analyses) were only found north of Point Conception, in the North Central and Central regions, and ranged in size from 6 km to 18 km long and 10 km^2 and 40 km^2 in area. These five mega features (one in the North Central and four in the Central region) possessed the typical coarse grain size, large bedforms, and distinct edges characteristics of RSDs, however, because they were often the dominant sediment type in the areas where they occur due to their large size, they were not always surrounded on all sides by a finer-grained sediment plateau and thus did not always exhibit the same depressed nature on all sides relative to this plateau as did the other RSD classes. Therefore, the processes governing the formation and maintenance of these numerically rare but extremely large features may differ somewhat from those associated with more typical RSD classes. When added into the distribution analysis, Mega RSDs made up 31% of the total RSD substrate classified state-wide, and influenced the depth distribution of the Central region.

6. Conclusion

The findings presented here provide a regional comparative overview of RSD substrate distribution and abundance along California's 1200 km long continental margin. RSDs were found along the entire length of the continental shelf, but with higher percent cover north of Point Conception. The majority of RSD substrate was concentrated between the 20 m and 80 m isobaths, with peak coverage at the 46 m isobath, which is consistent with previous site-specific RSD studies. The landscape analyses of RSD distribution on the continental shelf found significant relationships between RSD percent cover, shelf width, and proximity to bedrock reef substrate. There was no association between RSD percent cover and headlands. There was a dramatic increase in RSD size, cover, and depth north of Point Conception, possibly corresponding to differences in wave and current dynamics as well as higher abundance of bedrock reef substrate north of Point Conception.

These results, documenting RSDs as a widespread and abundant substrate along a significant portion of the western North American continental shelf, often comparable in percent cover to that of bedrock reef, suggests the need to include RSDs in habitat classification schemes for marine spatial planning initiatives such as the design and monitoring of MPAs. The ecological justification for such an addition is further supported by recent findings of highly significant biotic differences between RSD and non-RSD soft sediment benthic communities (Hallenbeck et al., 2012).

The results from this application of the CSMP bathymetric and acoustic backscatter data to quantify and classify patterns and landscape relationships in the distribution and abundance of RSD sets the stage for more detailed investigations into the processes associated with RSD formation, persistence, and change. These mechanisms likely include the interactions of storm events, large waves, sediment input, coastal and tidal currents, and other interactions with bathymetric features occurring at multiple spatial and temporal scales. The documented patterns of where RSDs tend to occur presented here will hopefully lead to the generation of new hypotheses regarding how they are formed and maintained, under what circumstances they change, and ultimately the placement of in situ process studies designed to test these hypotheses.

Acknowledgments

We thank the following members of the CSUMB Seafloor Mapping Lab P Iampietro, J Blakely, C Marks, J Gomez, J Carillo, P Consulo and C Bretz. We also thank R Jensen of the United States Army Corps of Engineers. Support for this work was provided by the California Ocean Protection Council's California Seafloor Mapping Program, the California State University Council on Ocean Affairs, Science and Technology, the CSUMB Undergraduate Research Opportunity Center, the CSUMB McNair Scholar's Program, and the US Geological Survey's Coastal and Marine Geology Program through the Pacific Benthic Habitats Project.

References

Anima, R.J., Eittreim, S.L., Edwards, B.D., Stevenson, A.J., 2002. Nearshore morphology and Late Quaternary geologic framework of the northern Monterey Bay Marine Sanctuary, California. Marine Geology 181, 35–54.

Auffret, G.A., Geistdoerfer, P., Gaillard, J.F., Reyes, J.L., Robouille, C., Voisset, M., Coutelle, A., Muller, C., Kerbrat, R., Monti, S., Ondreas, H., Mauviel, A., 1992. Caract´erisations´edimentologique et biologique pr´eliminaire des sites du projet EUMELI. Comptes Rendus de l'Académie des Sciences – Series II 314, 187–194.

Aubrey, D.G., Twichell, D.C., Pfirman, S.L., 1984. Holocene sedimentation in the shallow nearshore zone off Nauset Inlet, Cape Cod, Massachusetts. Marine Geology 47, 243–259.

Bagnold, R.A., 1946. Motion of waves in shallow water; interaction between waves and sand bottoms. Proceedings of the Royal Society of London, Series A: Mathematical Physical and Engineering Science 187, 1–15.

Bellec, V.K., Reidulv, B., Leif, R., Slagstad, D., Oddvar, L., Dolan, M., 2010. Rippled scour depressions on continental shelf bank slopes off Nordland and Troms, Northern Norway. Continental Shelf Research 30, 1056–1069.

Beyene, A., Wilson, J.H., 2007. Digital mapping of California wave energy resource. International Journal of Energy Research 31, 1156–1168.

Blanchette, C.A., Helmuth, B., Gaines, S.D., 2006. Spatial patterns of growth in the mussel, *Mystilus californianus,* across a major oceanographic and biogeographic boundary at Point Conception, California, USA. Journal of Experimental Marine Biology and Ecology 340, 126–148.

Bromirski, P., Cayan, D., Flick, R., 2005. Wave spectral energy variability in the northeast Pacific. Journal of Geophysical Research 110, 30–45.

Browder, A.G., McNinch, J.E., 2006. Linking framework geology and nearshore morphology: correlation of paleo-channels with shore-oblique sandbars and gravel outcrops. Marine Geology 231 (1–4), 141–162.

Brown, C.J., Collier, J.S., 2008. Mapping benthic habitat in regions of gradational substrata: an automated approach utilizing geophysical, geological, and biological relationships. Estuarine Coastal and Shelf Science 78, 203–214.

Cacchione, D.A., Drake, D.E., Grant, W.D., Tate, G.B., 1984. Rippled scour depressions on the inner continental shelf off central California. Journal of Sedimentary Petrology 54 (4), 1280–1291.

Cacchione, D.A., Field, M.E., Drake, D.E., Tate, G.B., 1987. Crescentic dunes on the inner continental shelf off northern California. Geology 15, 1134–1137.

Cacchione, D.A., Drake, D.E., 1990. Shelf sediment transport: an overview with applications to the northern California continental shelf. In: LeMehaute, B., Hanes, D. (Eds.), The Sea, Ocean Engineering Science. Wiley-Interscience, pp. 729–773.

California Department of Fish and Game, 2008a. California Marine Life Protection Act: Master plan for Marine Protected Areas.

California Department of Fish and Game, 2008b. California Marine Life Protection Act: Master plan for Marine Protected Areas, Appendix: G.

Coco, G., Murray, A.B., Green, M.O., Thieler, E.R., Hume, T.M., 2007. Sorted bedforms as self-organized patterns: 2. Complex forcing scenarios. Journal of Geophysical Research 112, 1–14.

Cohen, J., 1960. A coefficient of agreement for nominal scales. Education and Pyschological Measurement 20, 37–46.

Ellis, J.R., Rogers, S.I., Freeman, S.M., 2000. Demersal assemblages in the Irish Sea, St George's Channel and Bristol Channel. Estuarine Coastal and Shelf Science 51, 299–315.

ESRI (Environmental Systems Resource Institute). 2009. ArcMap 9.2. ESRI, Redlands, California.

Eittreim, S.L., Anima, R.J., Stevenson, A.J., 2001. Seafloor geology of the Monterey Bay area continental shelf. Marine Geology 181, 3–34.

Evans, O.F., 1942. The relation between the size of wave-formed ripple marks, depth of water, and the size of the generating waves. Journal of Sedimentary Research 12, 31–35.

Ferrini, V., Flood, R.D., 2005. A comparison of Rippled Scour Depressions identified with multibeam sonar: evidence for sediment transport in inner shelf environments. Continental Shelf Research 25, 1979–1995.

Field, M.E., Roy, P.S., 1984. Onshore transport and sandbody formation: evidence from a steep high-energy shoreface in southeastern Australia. Journal of Sedimentary Research 54, 1292–1302.

Garnaud, S., Leueuer, P., Garlan, T., 2005. Origin of rippled scour depressions associated with cohesive sediments in a shoreface setting (eastern Bay of Seine, France). Geo.-Marine Letters 25, 34–42.

Garrison, T., 2009. Essentials of Oceanography, fifth ed. Brooks/Cole, Cengage Learning, California.

Goff, J.A., Mayer, L.A., Traykovski, P., Buynevich, I., Wilkens, R., Raymond, R., Glang, R., Evans, R.L., Olson, H., Jenkins, C., 2005. Detailed investigation of sorted bedforms, or "rippled scour depressions" within the Martha's Vineyard Coastal Observatory, Massachusetts. Continental Shelf Research 25, 461–484.

Gray, J.S., 2002. Species richness of marine soft sediments. Marine Ecology Progress Series 244, 285–297.

Green, M., Vincent, C., Trembanis, A., 2004. Suspension of coarse and fine sand on a wave-dominated shoreface, with implications for the development of rippled scour depressions. Continental Shelf Research 24, 317–335.

Gutierrez, B.T., Voulgaris, G., Thieler, R.E., 2005. Exploring the persistence of sorted bedforms on the inner-shelf of Wrightsville Beach, North Carolina. Continental Shelf Research 25, 65–90.

Hallenbeck, T.R., Kvitek, R., Lindholm, J., 2012. Rippled scour depressions add ecologically significant heterogeneity to soft sediment habitats on the continental shelf. Marine Ecology Progress Series 468, 119–133.

Hequette, A., Hill, P.R., 1993. Storm-generated currents and offshore sediment transport on a sandy shoreface, Tibjak Beach, Canadian Beaufort Sea. Marine Geology 113, 283–304.

Hickey, B.M., 1993. In: Dailey, M.D., Reish, D.J., Anderson, J.W. (Eds.), Physical Oceanography; in Ecology of the Southern California Bight: A synthesis and Interpretation. University of California Press, pp. 19–70.

Holland, K.T., Elmore, P.A., 2008. A review of heterogeneous sediments in coastal environments. Earth-Science Reviews 89, 116–134.

Hunter, R.E., Dingler, J.R., Anima, R.J., Richmond, B.M., 1988. Coarse-sediment bands on the inner shelf of southern Monterey Bay, California. Marine Geology 80 (1–2), 81–98.

Iacono, C.L., Guillen, J., 2008. Environmental conditions for gravelly and pebbly dunes and sorted bedforms on a moderate-energy inner shelf (Marettimo Island, Italy, western Mediterranean). Continental Shelf Research 28, 245–256.

Lentz, S.J., 1994. Current dynamics over the Northern California inner shelf. Journal of Physical Oceanography 24, 2461–2478.

Lindholm, J., Auster, P., Valentine, P., 2004. Role of large marine protected area for conserving landscape attributes of sand habitats on Georges Bank (NW Atlantic). Marine Ecology Progress Series 269, 61–68.

Mariant, J., 1993. Origin of Sediment Ripple Bands and Zones on the Inner Shelf of Southern Monterey Bay, California. Master's thesis, San Jose State University. 77 pp.

Murray, B., Thieler, R.E., 2004. A new hypothesis and exploratory model for the formation of large scale inner-shelf sediment sorting and rippled scour depressions. Continental Shelf Research 24, 295–315.

Molnia, B.F., Schwab, W.C., Austin, W.W. 1983. Map of Potential Geologic Hazards on the Northern Aleutian Shelf (lease sale 92), Bering Sea. US Geological Survey Open File Report 83–247. 3pp.

Phillips, E., 2007. Exploring Rippled Scour Depressions Offshore Huntington Beach, CA. Master's thesis, University of California Santa Cruz. 58pp.

Puig, P., Ogston, A.S., Mullenbach, B.A., Nittrouer, C.A., Sternberg, R.W., 2003. Shelf-to-canyon sediment-transport processes on the Eel continental margin (northern California). Marine Geology 193, 129–149.

Patterson, D., 2010. Bounding Containers ArcScript for ESRI ArcMap 9.3 and 9.3.1. ⟨http://arcscripts.esri.com/details.asp?dbid=14535⟩.

Putnam, J.A., Johnson, J.W., 1949. The dissipation of wave energy by bottom friction. Transactions American Geophysical Union 30 (3), 349–356.

Reid Jr., J.L., Schwartzlose, R.A., 1962. Direct measurements of the Davidson current off Central California. Journal of Geophysical Research 67 (6), 2491–2497.

Reid, J.A., Reid, J.M., Jenkins, C.J., Zimmermann, M., Williams, S.J., Field, M.E., 2006. usSEABED – Pacific Coast (California, Oregon, Washington) offshore surficial-sediment data release. U.S. Geological Survey Data, Series 182, version 1.0. ⟨/http://pubs.usgs.gov/ds/2006/182/S⟩.

Reimnitz, E., Toimil, L.J., Shepard, F.P., Gutierrez-Estrada, M., 1976. Possible rip current origin for bottom ripple zones, to 30-m depth. Geology 4 (7), 395–400.

Seafloor Mapping Lab at CSUMB: SFML Data Library. Web. 08 Feb. 2011. ⟨http://seafloor.csumb.edu/SFMLwebDATA_SURVEYMAP.html⟩.

Shemdin, O., Hasselmann, K., Hsiao, S.V., Heterich, K., 1978. Nonlinear and linear bottom interaction effects in shallow water. Turbulent Fluxes through the Sea Surface, Wave Dynamics and Prediction. NATO Conf. Ser. 1, 347–365.

Short, A.D., 1996. The role of wave height, period, slope, tide range and embaymentisation in beach classifications: a review. Revista Chilena de Historia Natural 69, 589–604.

Snelgrove, P.V.R., Grassle, J.F., Petrecca, R.F., 1994. Macrofaunal response to artificial enrichments and depressions in a deep-sea habitat. Journal of Marine Research 52, 345–369.

Soulsby, R.L., Whitehouse, R.J.S., Marten, K.V., 2012. Prediction of time-evolving sand ripples in shelf seas. Continental Shelf Research 38, 47–62.

Storlazzi, C.D., Jaffe, B.E., 2002. Flow and sediment suspension events on the inner shelf of central California. Marine Geology 181, 95–213.

Storlazzi, C.D., Reid, J., 2010. The influence of El Niño-Southern Oscillation (ENSO) cycles on wave-driven sea-floor sediment mobility along central California continental margin. Continental Shelf Research 30, 1582–1599.

USACE, United States Army Corps of Engineers: Wave Information Studies. Web. 05 April 2012. ⟨http://wis.usace.army.mil/hindcasts.shtml?dmn=pac⟩.

Van Hoey, G., Degraer, S., Vincx, M., 2003. Macrobenthic community structure of soft-bottom sediments at the Belgian Continental Shelf. Estuarine Coastal and Shelf Science 59, 599–613.

Weiss, A., 2001. Topographic positions and landforms analysis. Proceedings of the Twenty-first Annual ESRI User Conference (Map Gallery Poster), San Diego, CA.

Winant, C.D., Beardsley, R.C., Davis, R.E., 1987. Moored wind, temperature, and current observations made during coastal ocean dynamics experiments 1 and 2 over the northern California continental shelf and upper slope. Journal of Geophysical Research 92, 1569–1604.

Wingfield, D.K., Storlazzi, C.D., 2007. Variability in oceanographic and meteorologic forcing along Central California and its implications on nearshore processes. Journal of Marine Systems 68, 457–472.